

University of Texas Rio Grande Valley

ScholarWorks @ UTRGV

---

Computer Science Faculty Publications and  
Presentations

College of Engineering and Computer Science

---

5-2020

## Using continuous sensor data to formalize a model of in-home activity patterns

Beiyu Lin

*The University of Texas Rio Grande Valley*

Diane J. Cook

Maureen Schmitter-Edgecombe

Follow this and additional works at: [https://scholarworks.utrgv.edu/cs\\_fac](https://scholarworks.utrgv.edu/cs_fac)



Part of the [Computer Sciences Commons](#)

---

### Recommended Citation

Lin, Beiyu, Diane J. Cook, and Maureen Schmitter-Edgecombe. 2020. "Using Continuous Sensor Data to Formalize a Model of In-Home Activity Patterns." *Journal of Ambient Intelligence and Smart Environments* 12 (3): 183–201. <https://doi.org/10.3233/AIS-200562>.

This Article is brought to you for free and open access by the College of Engineering and Computer Science at ScholarWorks @ UTRGV. It has been accepted for inclusion in Computer Science Faculty Publications and Presentations by an authorized administrator of ScholarWorks @ UTRGV. For more information, please contact [justin.white@utrgv.edu](mailto:justin.white@utrgv.edu), [william.flores01@utrgv.edu](mailto:william.flores01@utrgv.edu).

# Using Continuous Sensor Data to Formalize a Model of In-Home Activity Patterns

Abstract. Formal modeling and analysis of human behavior can properly advance disciplines ranging from psychology to economics. The ability to perform such modeling has been limited by a lack of ecologically-valid data collected regarding human daily activity. We propose a formal model of indoor routine behavior based on data from automatically-sensed and recognized activities. A mechanistic description of behavior patterns for identical activity is offered to both investigate behavioral norms with 99 smart homes and compare these norms between subgroups. We identify and model the patterns of human behaviors based on inter-arrival times, the time interval between two successive activities, for selected activity classes in the smart home dataset with diverse participants. We also explore the inter-arrival times of sequence of activities in one smart home. To demonstrate the impact such analysis can have on other disciplines, we use this same smart home data to examine the relationship between the formal model and resident health status. Our study reveals that human indoor activities can be described by non-Poisson processes and that the corresponding distribution of activity inter-arrival times follows a Pareto distribution. We further discover that the combination of activities in certain subgroups can be described by multivariate Pareto distributions. These findings will help researchers understand indoor activity routine patterns and develop more sophisticated models of predicting routine behaviors and their timings. Eventually, the findings may also be used to automate diagnoses and design customized behavioral interventions by providing activity-anticipatory services that will benefit both caregivers and patients.

## KEYWORDS

Human dynamics, Population modeling, Pareto distribution, Pervasive environment, Activity recognition

## 1 INTRODUCTION

The wealth of data that can now be collected by ambient sensors facilitates the development of new models of human behavior supported by empirical evidence. In this paper, we propose formal models of human activities for indoor environments. Specifically, we analyze and model the sequences and timings of basic everyday activities for smart home residents. Offering such models provides a basis for making claims regarding human behavior and differentiating behavior strategies for population subgroups (healthy, dementia). We validate our models by using multiple years of ambient sensor data collected in smart homes. We find that activity arrival rates can be mathematically modeled and that model parameters differ between healthy older adults and older adults with chronic health issues. These analyses allow researchers to better understand the impact of health conditions on routine behavior and can be used to predict diagnosis categories for individuals based on automatically-sensed activity patterns.

Due to limitations with real-world data collection methods, previous models for human activities did not provide sufficient information about the dynamic property of human behaviors. They typically assumed that human activities can be modeled by Poisson processes and that the inter-arrival time, or the time interval between two successive activities, follows an

exponential distribution. This assumption models activities as occurring at a constant rate [1]-[4]. However, this model does not capture the fluctuation that may occur in activity arrival rates. With the advent of quantifiable mobile data that can be collected unobtrusively and continuously, researchers recently proposed the use of heavy-tailed distributions to describe human dynamics [5]-[9].

Our approach in this paper is to build a general model of human activities that involves real-time data collection in everyday environments based on ambient sensor data collected in smart homes. We perform our data collection on subjects inside their own homes. The data collection reflects routine human behavior without requiring any alteration to the environment or activities, facilitating an ecologically valid analysis. We analyze the inter-arrival times of automatically-labelled smart home sensor data (e.g., cooking, eating), and find activity interdependencies in subgroups (healthy older adults and older adults with chronic health problems). To investigate the relationship between behavior changes and health problems, we use a case study with 65 months of data from one smart home. This behavior-driven sensor data shows that activity routines can be modeled by non-Poisson processes. The activity inter-arrival times follow a heavy-tailed distribution, specifically a Pareto distribution.

We find that model parameters for activity arrival rates differ between healthy older adults and older

1 adults with health issues. The resulting mathematical  
 2 models open up the possibility of recognizing the  
 3 development of health problems and providing efficient  
 4 interventions and assistance. Once differences in  
 5 patterns among subgroups are found, they can be used  
 6 to better understand the impact of culture, age, and  
 7 education on daily routines. The design of technology-  
 8 based tools such as agent- and human-oriented software  
 9 and hardware systems [8], [10]–[12] can also greatly  
 10 benefit from this work. Researchers in the fields of  
 11 sociology, psychology, and anthropology will also be able  
 12 to align their studies with customized and personalized  
 13 healthcare systems.

14 Our study provides evidence to support three  
 15 hypotheses of human routine behaviors in home  
 16 environments. First, human behavior can be described  
 17 by formal statistical distributions. Second, data  
 18 supporting this conclusion can be collected using  
 19 ambient sensors in an ecologically valid manner. Third,  
 20 the Pareto model and its properties, such as the 80/20  
 21 rule, can be useful for the study of human dynamics and  
 22 investigation of hypotheses because of its ability to  
 23 model human behavior patterns. Our study first analyzes  
 24 and models inter-arrival times of identical indoor  
 25 behaviors based on both 99 smart homes and subgroups  
 26 of older adults. We further study the inter-arrival times  
 27 of activity sequences from one smart home. The findings  
 28 of this study will offer the potential to automate  
 29 diagnoses and design customized behavioral  
 30 interventions.

## 31 2. LITERATURE REVIEW

32 Maturing pervasive computing technologies have  
 33 sparked a new wave of human behavior analysis and  
 34 resulted in new theories regarding human behavior  
 35 patterns. Barabási's study of the timing of consecutive  
 36 electronic and physical mail messages sparked a model  
 37 of human dynamics as a heavy-tailed distribution [5],  
 38 [13]. A queuing model and heavy-tailed distribution  
 39 were introduced in Barabási's study to explain the large  
 40 time gap between sent messages after a burst of  
 41 responses.

42 After Barabási's discovery, scientists use heavy-  
 43 tailed distributions to explain human behavior in diverse  
 44 domains, ranging from social science to health care. In  
 45 the social network field, heavy-tailed distributions are  
 46 used to characterize the dynamics of popularity based on  
 47 diverse digital platforms, such as Wikipedia, blog posts,  
 48 Android applications, Web pages, and Twitter [14]–[20].  
 49 As an example, Li et al. show that the behavior-based  
 50 popularity of Android applications follows the Pareto  
 51 principle [17]. Tsompanidis et al. also discover that web  
 52 traffic flow size can be explained by the Pareto  
 53 distribution [19]. Similarly, researchers presented a list

54 of social and organizational power laws, one kind of  
 55 heavy-tailed distribution, to describe human behavior  
 56 [21]–[23]. Specifically, the power law distribution  
 57 identifies the number of inter-firm relationships  
 58 observed from linkages between firms: suppliers,  
 59 customers, and owners [22], [23].

60 Further, scientists use heavy-tailed distributions to  
 61 model and predict human mobility [24]–[30]. For  
 62 example, GPS-based human movement patterns can be  
 63 captured by heavy-tailed flights for different  
 64 transportation modes, including walking/running and  
 65 car/taxi [28]–[30]. Regardless of transportation modes,  
 66 the distribution of user's moving distances, from visited  
 67 locations to the target location, can be modelled by the  
 68 Pareto distribution [27].

69 Besides heavy-tailed distributions, other  
 70 mathematical models are also used to understand a more  
 71 varied set of human activities than basic movements. A  
 72 mixture of Gaussian intensities model is introduced to  
 73 explain activities, such as exercising and eating, that have  
 74 time-varying, interdependent, and periodic properties  
 75 [31]. The temporal granularity algorithm, considering  
 76 behaviors happened within a time interval instead of at  
 77 an exact timestamp, is used to identify frequent  
 78 behavioral patterns, such as receiving a call,  
 79 sending/receiving a text message, and holding a meeting  
 80 [32].

81 In addition to mathematical formalisms, researchers  
 82 adopt machine learning methods to model aspects of  
 83 human behavior [33], [34]. For example, inverse  
 84 reinforcement learning (a method which flips the  
 85 problem of traditional reinforcement learning and learns  
 86 an agent's rewards by observing its behavior) models  
 87 human driving routines to help aggressive drivers  
 88 improve their driving style [33] and to find taxi driver's  
 89 preferences on working regions and times [34].

90 Given the development of these diverse models to  
 91 understand human behavior patterns, we propose to  
 92 extend previous work further by modeling indoor  
 93 behavior patterns based on ambient sensor data.  
 94 Although researchers have analyzed raw sensor data and  
 95 design features from the raw sensor data to understand  
 96 human behaviors in smart environments [35]–[38], the  
 97 substantial number and diversity of raw sensor event  
 98 patterns are difficult to provide a rich vocabulary to  
 99 express human behavior. Analyzing the labeled activities  
 100 from sensor event sequences resolves the concern.

101 In this paper, we model generalized human behavior  
 102 based on ambient sensor data collected in smart homes.  
 103 Other work has similarly focused on labeling and  
 104 analyzing smart home-based behavior. Some of this prior  
 105 research introduces data-driven techniques for  
 106 recognizing or predicting daily activities in smart home  
 107 environments based on continuous sensor data [39]–  
 108 [46]. Based on raw or activity-labeled sensor data, other

1 studies analyze and assess and individual’s physical and  
 2 mental health stated associated with the observed  
 3 behavior [47], [48]. Outside of the health domain,  
 4 researchers have also analyzed behavior patterns from  
 5 ambient sensor data to predict the associated energy  
 6 consumption [49], a useful step in designing energy-  
 7 efficient automated buildings. However, these  
 8 techniques do not offer a mechanistic description of  
 9 indoor behavioral patterns. Furthermore, they have not  
 10 yet attempted to describe behavior patterns at a  
 11 population level.

12 Our work explores several research problems. First,  
 13 we utilize activity recognition methods to label sensor  
 14 data in real time with corresponding activity labels.  
 15 Second, based on this labeled data, we analyze activity  
 16 inter-arrival times and construct heavy-tailed  
 17 distributions, specifically Pareto distributions, to  
 18 describe routine patterns for smart home residents in  
 19 everyday environments. Third, we investigate the  
 20 patterns of selected activities both at a group level with  
 21 99 smart homes and between subgroups of older adults  
 22 (healthy, chronic condition) to have a generalized  
 23 understanding of behavior patterns and their differences  
 24 across a population. Fourth, we analyze the information  
 25 from our model to determine its value as an indication of  
 26 a person’s health status.

### 27 3. METHODOLOGY

28 We propose a method to formally model activity  
 29 timings from behavior-based sensor data. First, we  
 30 monitor sensor events and automatically label the events  
 31 with corresponding activity names using machine  
 32 learning models [41]. We then use change point  
 33 detection (CPD) [50] to segment data into sequences that  
 34 represent single, uninterrupted activities. Once the data  
 35 is segmented, we apply a well-known statistical method,  
 36 extreme value theory (EVT) [28] to remove noise. We use  
 37 the remaining data to perform distribution fitting of the

53 histogram of activity inter-arrival times. We model the  
 54 data for 82 different probability distribution functions  
 55 (pdf) and determine the best distributions based on  
 56 minimizing the summation of the squared errors (SSE).  
 57 We utilize non-Poisson processes to model the inter-  
 58 arrival times of human behavior routines and postulate  
 59 that activity inter-arrival times can be approximated by  
 60 Pareto distributions. The modeling steps are illustrated  
 61 in Fig. 1.

62 We repeat these modeling steps for each activity  
 63 separately both for a complete sample of 99 smart home  
 64 residents as well as for two subgroups of older adults  
 65 within the sample: healthy and chronic cognitive or  
 66 physical health conditions. We test the hypothesis that  
 67 differences in health status between subgroups may be  
 68 significantly reflected by patterns of each activity.  
 69 Analyzing inter-arrival times for one activity at a time is  
 70 reflective of analysis techniques used in previous studies  
 71 [51]–[54]. Furthermore, focusing on a single activity  
 72 allows us to understand the potential relationship  
 73 between the activity of interest and population  
 74 subgroups as well as identify differences in model  
 75 parameters between activities. On the other hand,  
 76 analyzing individual activity may prevent us from  
 77 holistically examining a person’s entire behavior routine.  
 78 Thus, we additionally analyze the entire activity  
 79 sequence patterns for one of the smart homes.

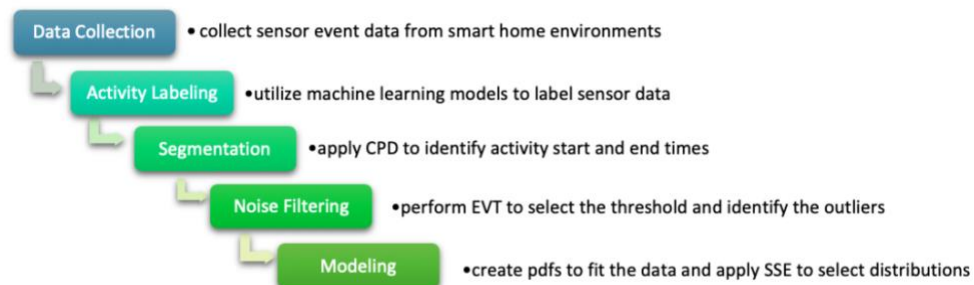
#### 80 3.1. Data Collection and Processing

81 In this study, we collect data from 99 smart homes to  
 82 investigate routine behavior patterns for selected  
 83 activities. We provide details on the first four steps of the  
 84 process in Fig. 1: data collection, activity labeling,  
 85 segmentation, and noise filtering.

##### 86 3.1.1. Data Collection

87 Data are collected using the CASAS Smart Home in a  
 88 Box (SHiB) [41], [55]. In each smart home, four types of  
 89 ambient sensors are installed: infrared motion, magnetic

on



49 Figure 1. The steps of population-based activity modeling. Ambient sensor data is collected from smart  
 50 homes, labeled with corresponding activities, and segmented. The data is cleaned then modeled based on  
 51 probability density functions to select appropriate distributions.

52

1 (door) contact, light level, and temperature level. These  
 2 sensors are discrete event sensors and thus only  
 3 generate a message (sensor event) when there is a  
 4 change in a state, such as a refrigerator door opening or  
 5 closing. The sensors are installed throughout the house  
 6 in each room including the kitchen, living room, dining  
 7 room, bedrooms, bathrooms, office, and laundry room.  
 8 Infrared motion sensors include narrow-area and wide-  
 9 area sensors. Narrow-area motion sensors detect heat-  
 10 based movements within a one-meter diameter area.  
 11 They are attached to the ceiling above specific objects or  
 12 areas in the home, such as above a participant’s favorite  
 13 chair or above a sink. Wide-area motion sensors perceive  
 14 movements occurring anywhere in an entire room.  
 15 These sensors are placed on ceiling corners in large  
 16 rooms, such as the dining or living room. Magnetic  
 17 sensors detect the use of doors and cabinets, such as in  
 18 entering or leaving the home or accessing items within  
 19 kitchen or bathroom cabinets. Temperature sensors can  
 20 be useful in detecting activities that change the heat level  
 21 in an area of the home, such as showering or cooking.  
 22 Similarly, light sensors can help us identify activities  
 23 occurring within a home as well as seasonal effects of  
 24 light levels.

25 3.1.2. Activity Labeling of Sensor Data

26 Activity labeling provides us with a rich vocabulary  
 27 to express human behavior. We employ automated  
 28 activity recognition techniques to label collected data  
 29 with eleven activity classes. The set of activities that we  
 30 categorize and use in this analysis are seven activities:  
 31 Relax, Cook, Eat, Personal Hygiene, Wash Dishes, Sleep,  
 32 and Work. We use a separate class, Other Activity, to  
 33 recognize unidentified sensor events.

34 We apply automated activity recognition (AR), a  
 35 heavily-investigated challenge [31], [34]–[38], to map a  
 36 sequence of captured sensor events onto one of the  
 37 activity classes. Our AR steps are based on an approach  
 38 that has been previously-validated for real-time activity  
 39 recognition from streaming sensor data [39]. First, we  
 40

55 extract features from the raw data collected from the  
 56 discrete event sensors (see Fig. 2). We move a fixed-size  
 57 sliding window over the time-ordered sensor data and  
 58 compute feature values for each window [33], [39], [40].  
 59 Within each window, sensor events may be widely  
 60 spread apart in time. To take this into account, a time-  
 61 based weighting factor is applied to account for the  
 62 relative temporal distance between sensor events.  
 63 Second, after training a random forest classifier with  
 64 ground truth pre-labeled sample data, the resulting  
 65 model can provide activity labels for data based on  
 66 features extracted from sensor sequences. The sequence  
 67 of sensor events in a window provides a context for  
 68 labeling the last (most recent) sensor event. The  
 69 approach we utilize is distinctive in that it is designed to  
 70 provide activity labels in real-time from ambient sensor  
 71 data collected continuously in real homes and to build a  
 72 generalizable model based on training ground truth-  
 73 labeled data. After training, the resulting model can  
 74 provide activity labels for data obtained in new smart  
 75 home settings. Our approach to activity recognition  
 76 yields an average of 95% accuracy and 0.78 F1 scores for  
 77 activity labeling based on the three-fold cross-validation  
 78 method [41].

79 After applying AR, all unidentified sensor events are  
 80 assigned to the class, Other Activity. The drawback of  
 81 putting all undefined activities into a single Other  
 82 Activity class is that we cannot distinguish those  
 83 activities from each other. Each of them may shed light  
 84 on the behavioral routines for the residents but because  
 85 they are grouped together, they cannot be analyzed as  
 86 individual activities. Therefore, for the Other Activity  
 87 category, we employ a k-means clustering algorithm to  
 88 divide the category into a specified number,  $k$ , of clusters.  
 89 The value of  $k$  is chosen using an elbow curve method,  
 90 which shows the minimized sum of squared distances of  
 91 samples from the closest cluster center. Thus, for each  
 92 home, our activity classes include both the seven  
 93 predefined and the cluster-generated activity classes,  
 94 which are labeled cluster<sub>1</sub> through cluster <sub>$k$</sub> .

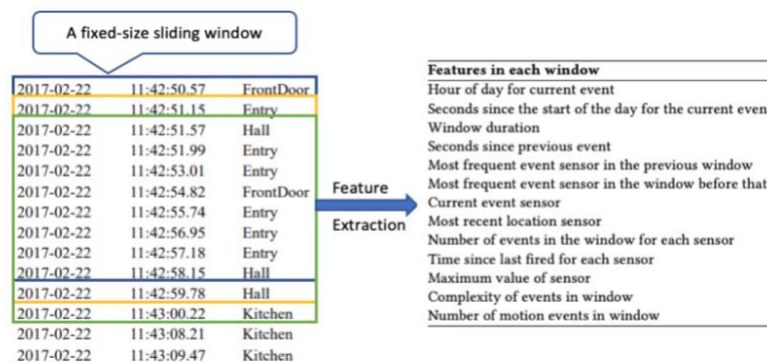


Figure 2. Using a fixed-size sliding window to extract features from the raw sensor data.

The activity recognition algorithm labels each sensor event with a corresponding activity class. The algorithm does not, however, indicate the beginning or ending of each activity occurrence. This information is valuable for our analysis because we want to consider the inter-arrival times of each activity's start as part of a person's overall routine. To segment labeled data into individual activities, we utilize an unsupervised method referred to as Change Point Detection (CPD). CPD identifies the point in time where the state of the underlying process changes [56], [57]. CPD can be used to detect real-time activity transitions or changes in the data between two successive windows of sensor events [58]. An example of sensor events with corresponding times, activity labels, and detected change points is shown in Fig. 3, where transitions are indicated by horizontal lines. The first event in an activity segment (the first sensor event after a change point) is considered the start of an activity and the last event in a segment (the last sensor event before a change point) represents the end of an activity. In this study, we use a CPD method that is based on Bayesian online learning [59]. Given the segmented data, we label each segment with the most majority activity label for that segment. The labeled activity in each segment provides us the time and activity information and allows us to calculate the inter-arrival times of each activity (in hours), defined as the time between two successive start times of the activity.

Change Point	Date and Time	Labelled Activity
0	2012-08-24 16:06:06	Other_Activity
0	2012-08-24 16:06:07	Other_Activity
1	2012-08-24 16:12:24	Other_Activity
0	2012-08-24 16:12:26	Relax
0	2012-08-24 16:13:34	Relax
0	2012-08-24 16:13:35	Relax
0	2012-08-24 16:34:52	Relax
0	2012-08-24 16:34:53	Relax
0	2012-08-24 16:35:05	Relax
0	2012-08-24 16:35:06	Relax
0	2012-08-24 16:35:06	Relax
0	2012-08-24 16:35:07	Relax
0	2012-08-24 16:35:10	Relax
0	2012-08-24 16:35:10	Relax
0	2012-08-24 16:35:13	Relax
0	2012-08-24 16:35:14	Relax
1	2012-08-24 16:35:17	Relax
0	2012-08-24 16:35:17	Relax

Figure 3. A sample of CPD application to the sensor data. A change point value of 1 indicates a transition/activity start time, 0 indicates no change. The 0 right before the next transition is the end time of an activity. A transition is detected and shown by a horizontal line.

### 3.1.3. Participant Information

In addition to collecting sensor data for 99 smart homes, we also store four additional parameters for each home: the number of residents as well as resident ages, education levels, and physical and mental health statuses (where available). Our sample includes single-resident (46%), two-resident (18%), three or more-resident homes (4%), and a not-reported category (32%). Residents can be categorized as young (age <35, 14%),

middle-aged (age 35-64, 9%), senior (age >64, 65%), and a not-reported category (12%). Education levels of residents in our dataset varies, including a high school diploma (10%), bachelor's degree (19%), master's level (20%), doctorate degree (15%), and a not-reported category (36%). Our entire 99 smart home dataset includes people who are healthy (57%) and those with targeted health ailments (23%) such as mild cognitive impairment (MCI) (9%), as well as those whose health status was not reported (20%).

While we have collected a large set of sensor data for this analysis, the data may not be representative of the population as a whole. Thus, we employ different indices to determine how representative our data are of the national population. Information statistics (Shannon index) and dominance (Simpson index) indices are utilized to identify and quantify both the richness (number of subgroups present) and abundance (the number of individuals per subgroup) of our smart home dataset in comparison with the US population. We also utilize mean and variance analysis to investigate the composition of the dataset. Further, we utilize Jaccard's coefficient index, a value between 0 (not similar) and 1 (identical), to compare the similarities between our smart home dataset and the US population. The data of the US population in 2010 is collected from the census government website [60]–[63].

For the information statistics, Fig. 4 shows that the value of Shannon indexes for age in our sample (1.01) is close to that at the national average (1.03), reflecting the richness and abundance of our smart home dataset. We further use the Simpson index to analyze the dominant subgroup (see Fig. 5) as well as mean and standard deviation to analyze the composition in both datasets (see Fig. 6). In Fig. 5, for the category of education level, both our smart home dataset and the national population have a Simpson index greater than 0.6, reflecting diverse education levels and no dominant subgroup. For age and number of residents, the Simpson index in our smart home dataset is less than 0.5 (dominant subgroups may exist). The mean and deviation charts (see Fig. 6) show that the mean value of age in our sample (76) is over twice that at the national level (37). In respect to household size, our sample does include fewer residents on average (1.4) than that in the national population (2.6). Our dataset is more representative of senior residents and low-population homes. The values of the Jaccard index for the categories of age(s), number of residents, and education level are 0.14, 0.14, and 1, respectively. That is, in the category of education level, our dataset is similar as the national population. A complete list of home descriptive parameters is provided in the supplementary material.

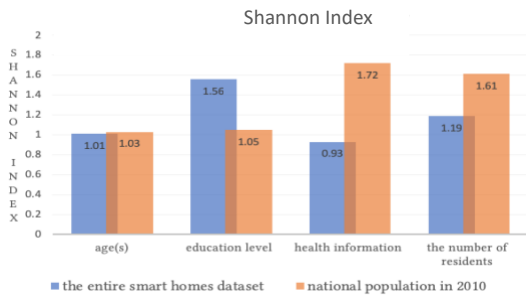


Figure 4. Shannon Index (information statistics index) of smart home dataset and national population in 2010.

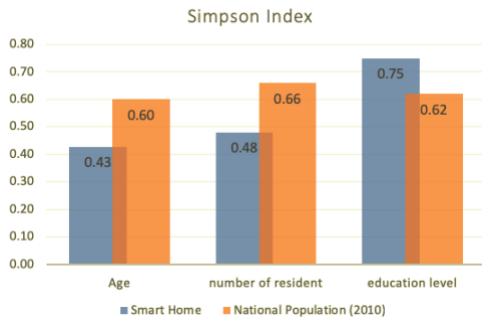


Figure 5. Simpson Index (dominance index) of smart home dataset and national population in 2010.

To analyze differences in behavior models between different population subgroups for individual activities, we select two subgroups among our smart home participants who are matched in terms of age and number of residents. The first subgroup consists of senior residents who are healthy and living alone (Subgroup H). This represents a baseline group for a comparison to senior residents who are living alone and have chronic health ailments. Most of these residents had multiple health problems. The most significant limiting conditions included mild cognitive impairment ( $N = 4$ ) and mild dementia ( $N = 3$ ). Further, one resident has Parkinson’s Disease, 4 people have mobility limitations, 2 residents have lung problems (chronic hypoxia/chronic obstructive pulmonary disorder), 2 participants have atrial fibrillation, and 1 resident has macular degeneration. To keep our sample sizes as large as possible, we did not constrain education level for these participants. There are 16 homes included in Subgroup H and 17 homes included in Subgroup NH. To study an entire sequence of activities, we selected a home with over five years of collected data. The resident of this selected home also experienced health changes during the data collection period. Specifically, the resident has vision and mobility problems.

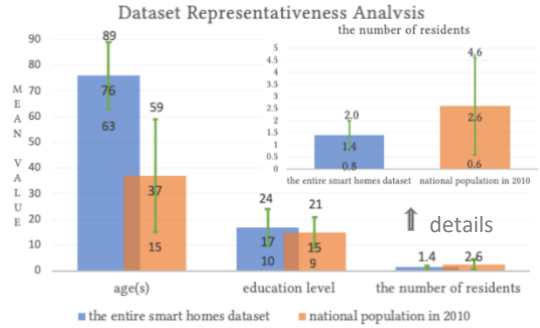


Figure 6. Mean and variance of each category from smart home dataset and national population in 2010.

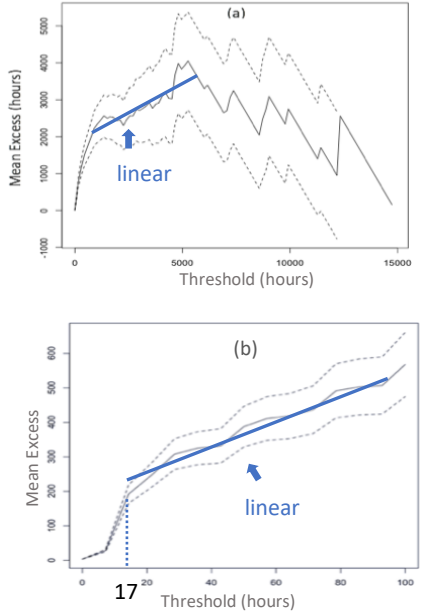
### 3.2. Data Cleaning

Before we fit a model to our smart home data, we preprocess the inter-arrival times of activity segments to remove noise. Noise can arise in smart home data due to issues including sensor failure, visitors in the home, activity recognition/segmentation errors, or changes that are made to the environment. While some of the outliers may represent behavioral changes that need to be captured, others represent errors in the data collection process and are best removed.

Our study focuses on large sets of continuous real-valued data. Longitudinal data collected from real homes is also subject to noise resulting from imperfect sensors and related system issues. As a result, we first apply outlier detection to the activity inter-arrival times by using a threshold exceedances approach, a principal approach found in extreme value theory (EVT). This approach allows us to test a range of threshold values  $u$  and identify outliers which have values above the threshold. For each candidate threshold, we fit a distribution for the excesses, the difference between the outlier and the threshold. Lower thresholds tend to bias the excess model by categorizing a large amount of data as outliers. Higher thresholds lead to a greater variance of the excess distribution because of the small number of outliers. The standard rule is to choose a threshold as low as possible so that the excesses fit a reasonable distribution [64], [65].

Here, a reasonable distribution is governed by two factors. First, we strive for a balance between bias and variance of the excesses distribution. Mean residual life plots help visualize this balance. A mean residual life plot graphs the mean value of excesses as a function of the threshold value. We select the threshold value at the lowest threshold value to show linearity in the plot. Linearity indicates that the bias and variance of the excess distribution are nearly evenly balanced. As an example of this approach, Fig. 7 shows the mean residual life plot with 95% confidence intervals for the inter-arrival times of the “Personal Hygiene” activity for our

1 sample of 99 homes. In Fig. 7(a), the x-axis shows a range  
 2 of threshold values ( $u$ ) from the minimum to the  
 3 maximum values observed Personal Hygiene inter-  
 4 arrival times. The y-axis shows the mean excess (the  
 5 mean of the excess times above the threshold) for each  
 6 threshold value.

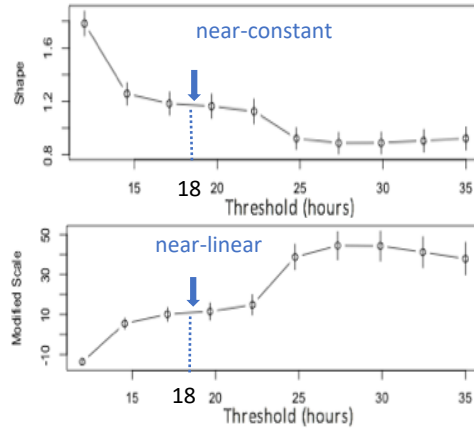


7  
8  
9  
10  
11  
12  
13  
14  
15  
16  
17  
18  
19  
20  
21  
22  
23  
24  
25  
26  
27  
28  
29  
30 Figure 7. (a) The mean residual life plot of Personal  
 31 Hygiene inter-arrival times for the entire dataset. Dashed  
 32 lines represent the 95% confidence interval. The solid  
 33 line plots the threshold value against the mean excess.  
 34 Both the threshold and excess values are in hours. The  
 35 graph is near-linear at  $u = 1000$  hours; (b) The mean  
 36 residual life plot of the Personal Hygiene inter-arrival  
 37 time for a range of thresholds from 5 to 20. Dashed  
 38 lines represent the 95% confidence interval. The solid  
 39 line represents the threshold value against the mean of  
 40 excesses. This graph is near-linear at  $u = 17$  hours.

41  
42 To balance the bias and variance of the excess  
 43 distribution, we identify a threshold value where the  
 44 solid line in Fig. 7(a) shows linearity. We notice that the  
 45 graph appears to be approximately linear around  $u =$   
 46  $1000$  hours. Since the value at the 99<sup>th</sup> percentile of the  
 47 entire dataset of the inter-arrival time of Personal  
 48 Hygiene is 13.1 hours, the value 1000 (hours) can be  
 49 considered a high threshold. To reduce the variance of  
 50 excess model fitting, we choose a threshold based on a  
 51 mean residual life plot for a range of thresholds from 5 to  
 52 20 (hours) as shown in Fig. 7(b). This plot suggests an  
 53 upper threshold (the maximum inter-arrival times) of  
 54 approximately 17 hours with 2835 outliers out of  
 55 366,441 data points, or 0.774% of the total number of  
 56 data points.

57 In the second step, we refine the threshold choice to  
 58 ensure that the shape parameter (affecting the shape of

59 a distribution instead of shifting or stretching/shrinking  
 60 the distribution) and modified scale parameter (affecting  
 61 the stretching/shrinking of a distribution) of the excess  
 62 distribution are quantifiably stable. To do this, we select  
 63 the lowest threshold value, near the approximated  
 64 threshold from the first step, for which both the  
 65 estimated shape parameter remains near-constant and  
 66 the estimated modified scale parameter is near-linear  
 67 [64].



68  
69  
70  
71  
72  
73  
74  
75  
76  
77  
78  
79  
80  
81  
82  
83  
84  
85 Figure 8. Parameter estimates against a range of  
 86 thresholds from 10 to 35 hours from the Personal  
 87 Hygiene inter-arrival times. We select the lowest value ( $u$   
 88  $= 18$  hours, the maximum inter-arrival times) of  
 89 thresholds, near the approximated threshold ( $u = 17$   
 90 hours, the maximum inter-arrival times), for which the  
 91 estimated shape (affecting the shape of the distribution  
 92 rather than shifting or stretching/shrinking it)  
 93 parameter remains near-constant and the estimated  
 94 modified scale (affecting the stretching/shrinking of a  
 95 distribution) parameter is near-linear.

96  
97 Using the same example of Personal Hygiene inter-  
 98 arrival times as in the first approach, Fig. 8 shows shape  
 99 and re-parametrized scale parameters as a function of  
 100 alternative threshold values. Based on the plots in Fig. 8,  
 101 which offer a model-based analysis of excess, we choose  
 102 a threshold of  $u = 18$  hours (the maximum inter-arrival  
 103 times) with 2730 outliers out of 366,441 data points  
 104 (0.745%). The perturbations among the excesses are  
 105 small relative to sampling errors based on the stability of  
 106 parameter estimates in Fig. 8.

107 **4. MODEL FITTING**

108 Modeling human behavior from smart home sensors  
 109 provides a unique perspective not only to investigate  
 110 behavioral norms but also to compare these norms  
 111 between population subgroups. Once differences in  
 112 patterns are discovered, they can be used to better  
 113 understand the impact of personal characteristics, such



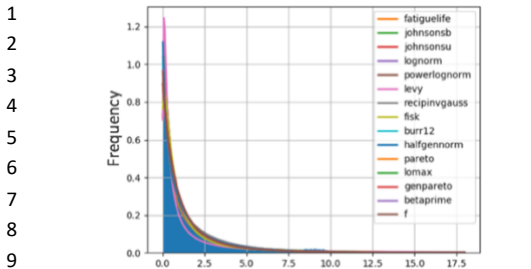
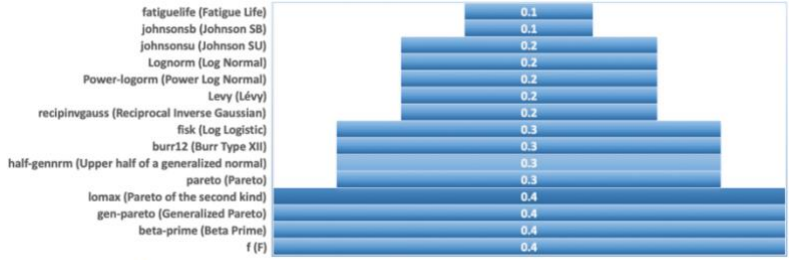


Figure 9. The top 15 fitted distributions, selected by SSEs, among 82 probability distributions.

as age, health conditions, and education on daily routines. They can also be used to automate diagnoses and predict additional behavioral features of individuals within a group. In this section, we provide details of our model fitting procedures. To illustrate the process, we focus on the Personal Hygiene activity observed from all the sampled smart homes.

We use the data below the selected EVT threshold to determine which distribution best describes the sensor-based activity data. We model data histograms using 82 different probability distribution functions. In our study, we employ the Freedman–Diaconis (F-D) rule to select the size of the bins for the histogram. In general, three well-known rules are used to calculate bin widths: the Sturges, Scott, and F-D rules. The Sturges rule is applicable when the data is from symmetric and Gaussian distributions [66]. The Scott rule works well for non-Gaussian distributions but refers to sample sizes between 50 and 500. For larger samples as in our study, the Scott rule estimates a smaller number of histogram bins, leading to over-smoothing. Over-smoothed histograms provide limited information on the shape of the underlying distribution [67]. The F-D rule is a robust method that substitutes the estimated standard deviation in the Scott rule with a multiple of the interquartile range. Thus, the F-D rule ensures 35% more bins than from the Scott rule as well as keeps the property of the Scott rule for non-Gaussian distributions [68], [69].

Next, we use the smallest summation of the square errors (SSE) value to compare distributions and select the distributions that best fit the data. SSE is calculated by determining the difference between the data and the fitted distribution. Here, we give an example of the distribution fitting and selection process for the Personal Hygiene inter-arrival times from all smart homes. The results of modeling the remaining activities and comparing the two subgroups are provided as supplementary material. While we use 82 distributions to fit the histogram, Fig. 9 shows the top 15 fitted distributions for the Personal Hygiene inter-arrival times from all the smart homes. The Pareto distribution is selected as one of these top distributions. Fig. 10



The SSE values for the top 15 fitted distributions. Smaller SSE indicates a better fit.

Figure 10. The SSE values for the top 15 fitted distributions. Smaller SSE values indicate a better fit.

summarizes the SSEs between the smart home data and the top 15 fitted distributions. The Pareto distribution has the same order-of-magnitude errors ( $10^{-1}$ ) as the other top distributions. We hypothesize that the Pareto distribution provides a close approximation to the top fitted distribution for Personal Hygiene inter-arrival times based on the sampled 99 smart homes. We test this hypothesis by both visualizing the fitting and determining the significance of the difference in fit between the Pareto distribution and the top-fitting distribution.

First, the figure on the left side of Fig. 11 shows the fit of the Pareto distribution and the top-fitting distribution for the Personal Hygiene inter-arrival times across all smart homes. Figures on the right side, (b) and (c), of Fig. 11, respectively, show portions of the fitted Pareto distribution for the Personal Hygiene inter-arrival times from 0 to 6.5 (hours) and from 3 to 18 (hours). Based on Fig. 11, the fitted Pareto distribution well approximates the shape of the histogram of the Personal Hygiene inter-arrival time in the entire dataset,

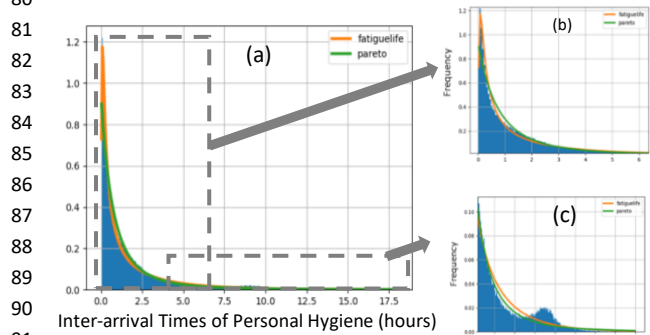


Figure 11. (a) Distribution fitting between the Pareto distribution and the top-fitting distribution. Bins are indicated by the x-axis. The y-axis represents frequency, the amount of data included in each bin divided by the total amount of data. The SSE of this Pareto distribution is 0.3. (b) Portion of the graph corresponding to shorter inter-arrival times (from 0 to 6.5 hours). (c) Portion of the graph corresponding to longer inter-arrival times (from 3 to 18 hours).

1 though the distribution did not capture everything from  
 2 the histogram. For example, a hump exists (see Fig. 11  
 3 (c)) around hours 8 through 10 with frequencies 0.01 to  
 4 0.02. Because, we are capturing a general view of indoor  
 5 behavior patterns rather than modeling each detail of a  
 6 single activity, we may also be observing overfit.

7 Second, to validate that the Pareto model provides a  
 8 statistically significantly-similar fit to the top-fitting  
 9 distribution, we perform a t-test analysis with the null  
 10 hypothesis that the two distributions have identical fit  
 11 scores. Given the activity inter-arrival times and the  
 12 estimated distribution parameters, we generate the  
 13 values of probability density functions for the Pareto  
 14 distribution and the top-fitted distribution. Next, we split  
 15 the two sets of values into 60 subsets and perform a  
 16 paired t-test on the means for each subset.

17 For Personal Hygiene inter-arrival times across all  
 18 sampled homes, the p value is 0.153 with the t-statistic -  
 19 1.443. For the null hypothesis that the two distributions  
 20 have identical average scores, a small p value ( $\leq 0.05$ )  
 21 leads to rejecting the null hypothesis and a large p value  
 22 ( $> 0.05$ ) leads to accepting the null hypothesis. Thus, we  
 23 accept the null hypothesis, and the Pareto distribution  
 24 can be considered approximately as strong as the top-  
 25 fitting distribution for the Personal Hygiene inter-arrival  
 26 times from the entire collection of smart homes. Similar  
 27 results were observed for all selected seven activities.

28 Based on both the visualization and t-test, the Pareto  
 29 distribution provides a strong fit for this activity data and  
 30 the properties of the Pareto distribution, for example the  
 31 80/20 rule, provide opportunities for future analyses  
 32 and investigations of hypotheses that model indoor  
 33 behavior patterns.

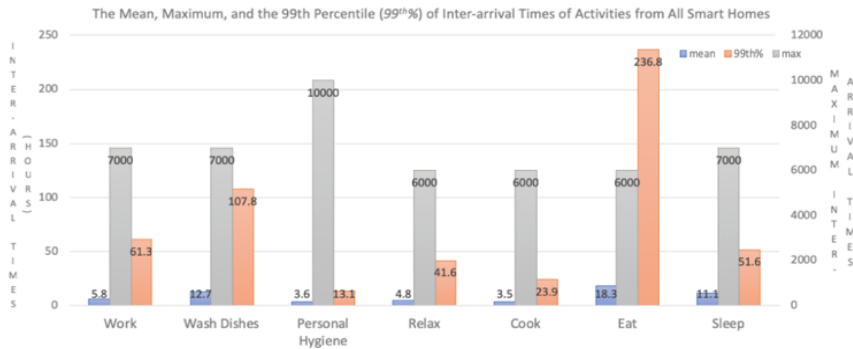
34 **5. RESULTS**

35 To understand the general principles behind human  
 36 behavior in everyday environments and to compare the

37 behavioral norms between population groups, we  
 38 perform the same procedures described in Sections 3  
 39 and 4 for each recognized activity both across all 99  
 40 smart homes and among two older adult subgroups  
 41 (Subgroup\_H and Subgroup\_NH). In addition, using the  
 42 same procedures as in Sections 3 and 4, we study a  
 43 holistic behavior routine in one home as a combination  
 44 of all detected activities.

45 For the data from 99 smart homes, before  
 46 performing outlier detection on the inter-arrival times of  
 47 each activity, we visualize some statistics to gain an  
 48 intuitive understanding of the data (see Fig. 12). In these  
 49 graphs, we observe that the maximum value of the inter-  
 50 arrival times of each activity is relatively large ( $\geq 10^3$   
 51 hours). There are multiple possible explanations for  
 52 these large values, including sensor failures and the  
 53 resident's absence from the home during travel. The 99<sup>th</sup>  
 54 percentile of inter-arrival times for each activity is in the  
 55 range of  $10^1$  to  $10^2$  hours. That is, approximately 99% of  
 56 occurrences for each activity exhibit small inter-arrival  
 57 times, thus only the top 1% of inter-arrival times  
 58 demonstrate these large values of interest. The mean  
 59 inter-arrival time for each activity is in the range of  $10^0$   
 60 to  $10^1$  hours. For example, the mean value of the inter-  
 61 arrival times of two successive Cook activities from 99  
 62 smart homes is 3.5 hours, which gives us a generalized  
 63 view about the gap between two successive Cook  
 64 activities. In Fig. 13, we notice that over 99.5% of the data  
 65 are kept after removing outliers. In addition, the  
 66 threshold value of each activity is above their mean value  
 67 (except activity Eat) and sometimes above the 99<sup>th</sup> %.

68 After filtering the outliers (using methods described  
 69 in Section 3), we perform model fitting as described in  
 70 Section 4. The summarized result of fitting of activity  
 71 inter-arrival times is shown in Fig. 14 and Table 1. In Fig.  
 72 14, we noticed that the shape parameter of the Pareto  
 73 distribution for Sleep inter-arrival times from the entire  
 74 smart home dataset is less than one. This means that the



88 Figure 12. A summary of inter-arrival times of all activities for all smart homes before performing outlier detection. The  
 89 results include the mean value of the dataset (mean), the 99th percentile (99<sup>th</sup>%) and maximum value of the dataset  
 90 (max).

91

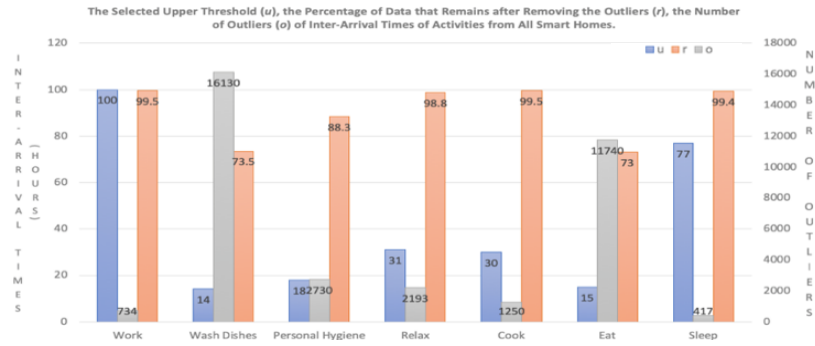


Figure 13. Summarized results of all activities for all smart homes. The results include the selected upper threshold ( $u$ ), the percentage of data that remains after removing the outliers ( $r$ ), and the number of outliers ( $o$ ).

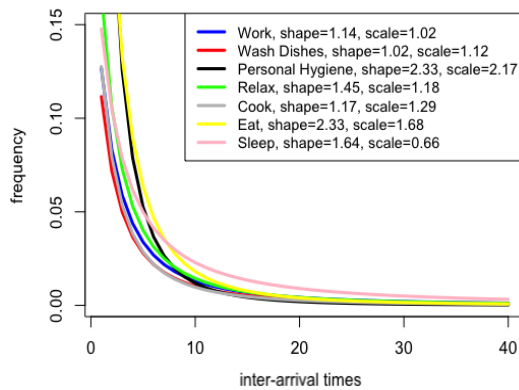


Figure 14. The Pareto distribution of each activity given simulated inter-arrival times from 0 to 40 hours.

expected start time of a Sleep activity relative to the previous Sleep occurrence approaches infinity. This result occurs because the mean value of the dataset is influenced by the largest single value. This may occur in finite-size samples when an outlier causes the mean to become arbitrarily large. The Sleep activity arrival times therefore cannot be adequately captured by distributions and thus we will use quantiles to describe the data spread of the Sleep activity.

Based on Fig. 15, we observe that for each activity, the SSE of the Pareto distribution fit is relatively small, in the range of  $10^{-3}$  to  $10^{-1}$ . Furthermore, the Pareto distribution for each activity is approximately as strong as the top-fitting distribution based on the large t-test p values ( $\geq 0.05$ ) in Table 1 (the null hypothesis is that the

two distributions have identical mean scores).

To further interpret the behavioral norms, we compare the selected thresholds ( $u$ ) and the Pareto shape parameters ( $\alpha$ ) for the entire sampled population and among population subgroups (see Figures 16 and 17). In Fig. 16 (a), the threshold of the inter-arrival time of Work, Relax, Cook, Eat, and Sleep in Subgroup NH is smaller than the corresponding threshold in Subgroup H.

One possible explanation for this difference is that individuals in Subgroup NH may be unable to sustain long periods of one activity, thus creating bursts of activities with short breaks. The phenomena might be due to physical health ailments, such as mobility or stamina difficulties that may require periods of rest. In addition, participants with cognitive limitations may be more likely to get distracted or experience difficulty remembering to quickly return to a task following an activity interruption, resulting in the need to reinitiate an activity within a short period of time.

Fig. 17 owns the values of the shape parameters of the Pareto distributions for the individual selected activities, the variations of which may be due to variations in health conditions. In Fig. 17(a), we observe that the shape parameters for activities Personal Hygiene, Relax, Cook, and Sleep in Subgroup H are smaller than the shape parameters in Subgroup NH. The smaller the shape parameter, the heavier the tail is of the Pareto distribution. That is, longer starting times between two successive activities occur more frequently in Subgroup H, possibly due to fewer interruptions.

Table 1. The p value of the t-test between the top-fitting distribution and the Pareto distribution ( $p$ ).

	Top Distribution	Fitted p value	Top Distribution	Fitted p value
Work	Burr	0.540	Relax	Inverse Gaussian
Wash Dishes	Fatigue life	0.312	Cook	Lévy
Personal Hygiene	Fatigue life	0.153	Eat	Fatigue life

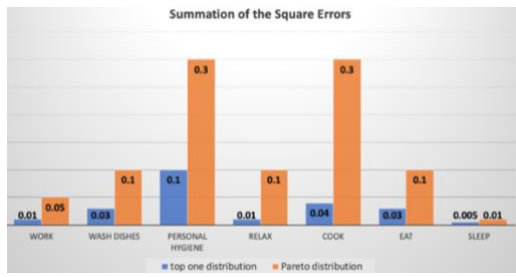


Figure 15. The SSE values of the top-fitting distribution and the fitted Pareto distribution.

Based on the above observations, we hypothesize that activity inter-arrival times may be used to predict subgroup classifications. We also notice that the Work activity (typically working at a desk or on a computer in an office area of the home) exhibits a large difference (0.36) in model shape parameters between the subgroups. To predict subgroup classifications, we currently use Work inter-arrival times from both subgroups and then utilize a random forest algorithm with 10-fold cross validation. The average accuracy of predictions is 0.814 and the standard deviation is 9.5. The precision of predicting subgroup classification is 0.784 and the recall is 0.740.

Further, to validate that the random forest algorithm provides a statistically significantly-better prediction than that from random guesses, we perform a t-test analysis with the null hypothesis that the mean difference of the prediction results from the two algorithms are equal to zero. The p value of the t-test is 0.0001 with the t-statistic 10.43. Since a small p value ( $\leq 0.05$ ) leads to rejecting the null hypothesis, we conclude that the prediction results from the random forest classifier using model parameter attributes are statistically significantly-better than those from random guesses. These results indicate that the formal model does indeed reflect differences in behavior patterns or population subgroups and can help us understand behavioral impacts of traits such as chronic health conditions.

In addition, the shape parameters for activities Wash Dishes, Personal Hygiene, Cook, and Eat in the combined dataset are larger than parameters for either of the subgroups. That is, the shorter starting times between two successive activities occur more frequently in the combined dataset. This may be due to the number and diversity of residents in the combined dataset. Homes with multiple residents, young, or middle-age residents have a higher frequency of shorter inter-arrival times than that for single senior residents. We also noticed that the shape parameter of Work in the combined dataset is smaller than either of the subgroups (larger gaps between two successive Work activity occurrences in the combined dataset exist), possibly

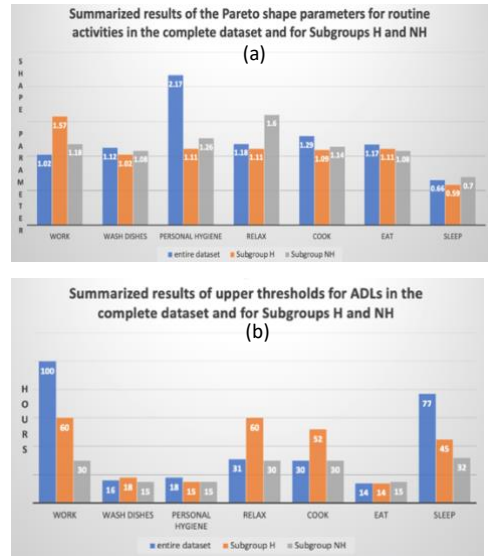


Figure 16. Summarized results of upper thresholds for ADLs in the complete dataset and for Subgroups H and NH. (a) Upper thresholds as a function of activity category. (b) Upper thresholds as a function of the subgroup.

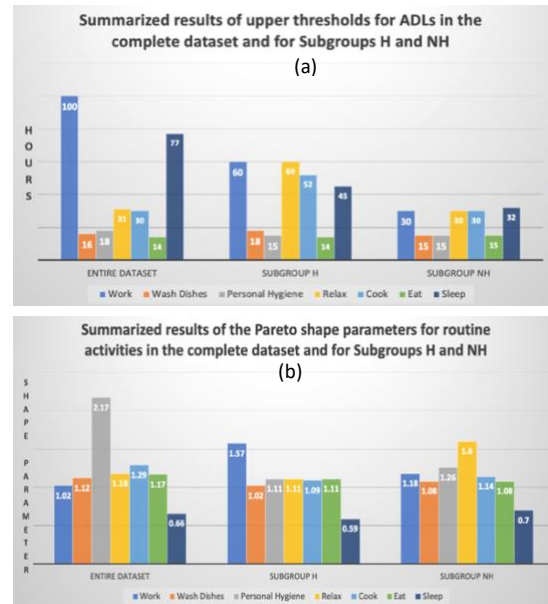


Figure 17. Summarized results of the Pareto shape parameters for routine activities in the complete dataset and for Subgroups H and NH. (a) Pareto shape parameters as a function of activity category. (b) Pareto shape parameters as a function of the subgroup.

due to the fluctuation of residents' schedules, such as when the residents' are travelling, while seniors often have more stable schedules.

In Fig. 17(b), we observe that in the combined dataset, the activities Relax and Eat have approximately the same value of the shape parameters (1.18 and 1.17, respectively). In Subgroup NH, activities Wash Dishes and Eat share the same value of the shape parameter (1.08 for both). In Subgroup H, four activities, Personal Hygiene, Relax, Cook, and Eat, have almost the same values of the shape parameters (1.11, 1.11, 1.09, and 1.11, respectively). Given the similar shape parameters, we propose to utilize bivariate or multivariate Pareto distributions (its cumulative density functions are shown in equations 1-3) to describe the combination of activities in each group. That is, the interdependencies of certain activities exist both at 99 smart homes and among subgroups. For example, in Subgroup NH, we can use a bivariate Pareto distribution to describe the relationship between activities Wash Dishes and Eat. In our study, all Pareto distributions are Pareto Type II.

consequently in model parameters) for healthy and non-healthy subpopulations given the activities we examined. However, using the models to automate diagnoses is left for future work.

$$F_{entire}(x_{work}, x_{eat}) = \left(1 + \frac{x_{relax} + 1.14}{1.14} + \frac{x_{eat} + 1.61}{1.61}\right)^{-1.17} \quad \text{Equation 1}$$

$$F_{subgroupNH}(x_{washDishes}, x_{eat}) = \left(1 + \frac{x_{washDishes} + 1.31}{1.32} + \frac{x_{eat} + 1.17}{1.17}\right)^{-1.08} \quad \text{Equation 2}$$

$$F_{subgroupH}(x_{personalHygiene}, x_{relax}, x_{cook}, x_{eat}) = \left(1 + \frac{x_{personalHygiene} + 1.66}{1.70} + \frac{x_{relax} + 2.96}{2.97} + \frac{x_{cook} + 1.66}{1.66} + \frac{x_{eat} + 1.33}{1.33}\right)^{-1.11} \quad \text{Equation 3}$$

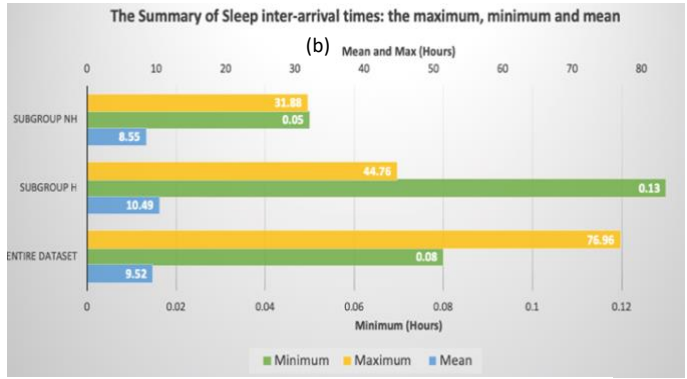
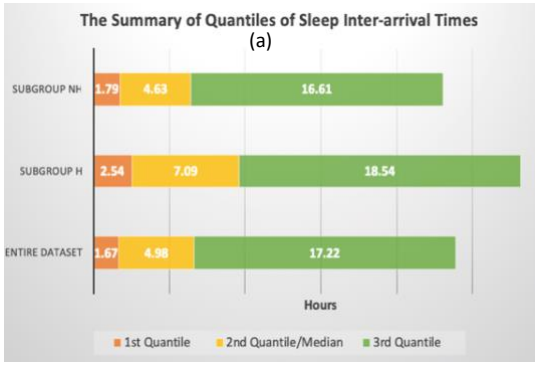


Figure 18. Summarized results of Sleep inter-arrival times. (a) includes the first quantile (1st Qu.), the median value (Median) / 2nd quantile (Median), the third quantile (3rd Qu.). (b) includes the minimum value of the dataset (Min.), the mean value (Mean), maximum value of the dataset (Max.).

The previous activities were tightly modeled as Pareto distributions. For Sleep inter-arrival times, the shape parameters are less than one for the entire sample of 99 smart homes and among population subgroups (see Fig. 17(a)). Statistically, this implies that the expected inter-arrival time approaches infinity. This result occurs because the mean value of the dataset is influenced by the largest value of the dataset. For a dataset of finite size, the sample has a finite value and so does the mean. But the more samples we have, the larger value of the mean. That is, the estimate of the mean is divergent when the size of the dataset goes to infinity. Since we cannot find a fitted distribution to adequately describe the pattern of the Sleep data below the selected thresholds, we utilize quantiles to understand the data spread (see Fig. 18). We notice that all the values in Subgroup H are greater than those in Subgroup NH. This is likely because residents with health ailments tend to experience more interrupted sleep. As this discussion highlighted, we do see differences in behaviour (and

Studying activity classes separately cannot provide a comprehensive view of a person’s entire routine. To understand all activities comprising a routine, we select one home to investigate patterns of all activities. We combine both the predefined (and labelled) seven activities and the remaining clustered activities. The appropriate number of clusters is selected when no significant change of the sum of squared distances occurs in the elbow curve. That is, the optimal number of clusters is near the elbow part of the curve. Based on Fig. 19, we select  $k = 10$ . The resident is a single senior whose health status transitioned from healthy to having vision and mobility problems during the course of data collection. The time period of the experiment for this home is 65 months (from 2011-06-14 to 2016-11-10).

We perform the same process of data processing and model fitting as described in Sections 3 and 4. Fig. 20 shows that the Pareto distribution also fits the inter-arrival times for all routine activities. The threshold and shape parameter of the inter-arrival times of all activities

1 are 5.8 hours and 1.17, respectively. The sum of square  
 2 error for the fitted Pareto distribution is 1.8. Given the  
 3 values of the shape (1.17) and scale (0.29) parameters,  
 4 we confirm that 17% of the total number of inter-arrival  
 5 points, which occurs in the tail, comprises 80% of the  
 6 total inter-arrival hours, and 20% of the total number of  
 7 inter-arrival points, comprises 74% of the total inter-  
 8 arrival hours.

9 To further investigate the relationship between the  
 10 fat tail of the Pareto distribution and the resident's health  
 11 status, we first look at the 20% of inter-arrival times that  
 12 occur in the tail and represent the large gap between two  
 13 successive activities, and then manually examine the  
 14 sensor data that corresponds to these gaps. Our  
 15 investigation is summarized in Fig. 21. We notice that the  
 16 successive activities, Sleep and Bed-Toilet Transition,  
 17 occur in 40% of the cases lying in the tail. We hypothesize

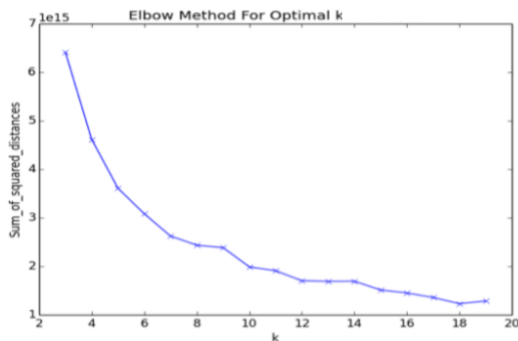


Figure 19. Elbow Curve.

55 that the large gap and high frequency of these two  
 56 activities are symptomatic of the resident's health  
 57 problems. We validate the hypothesis by comparing the  
 58 provided health information with the sensor-based night  
 59 time walking duration (minutes) for the corresponding  
 60 dates (see Fig. 22). Average night time walking duration  
 61 is calculated based on the time that elapses between the  
 62 end of a sleep activity and the beginning of the following  
 63 bed toilet transition, given that the distance between bed  
 64 and bathroom is constant and night-time bathroom trips  
 65 typically involve direct routes.

66 We observe an increase in the average walking  
 67 duration from August 2014 to November 2014. Self-  
 68 reported mobile difficulty also increases during that  
 69 time, provide a possible explanation for this change. We  
 70 also notice that from December 2014 to March 2015 the  
 71 sensor data reflects a decrease in the average walking  
 72 duration, while the self-reported mobility difficulty

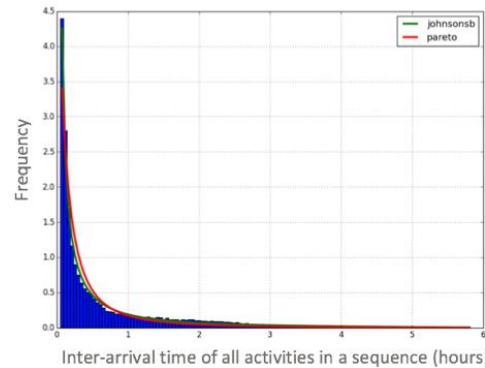


Figure 20. The Pareto distribution and the top-fitting distribution.

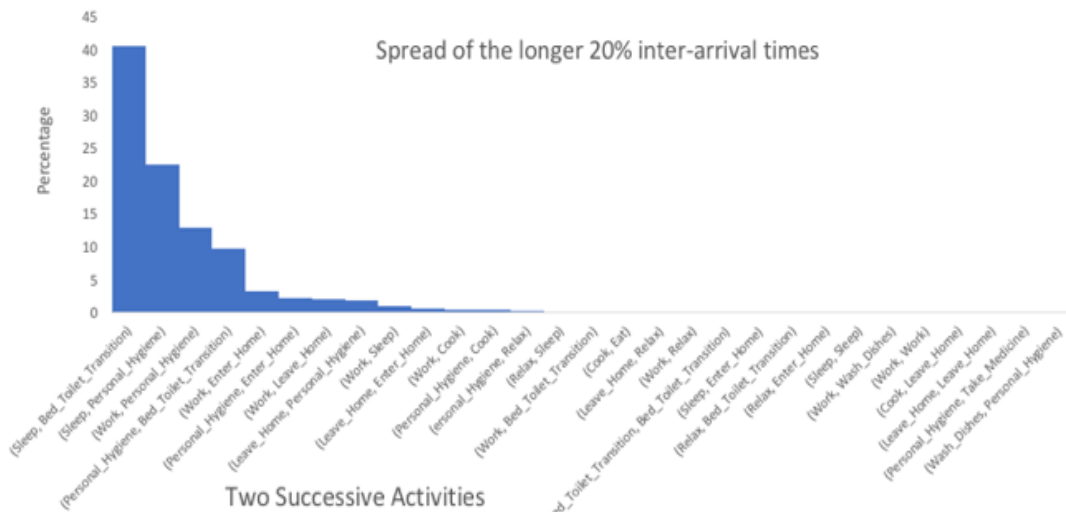


Figure 21. Spread of the two successive activities in 20% of the total inter-arrival times that occur in the tail of the distribution.

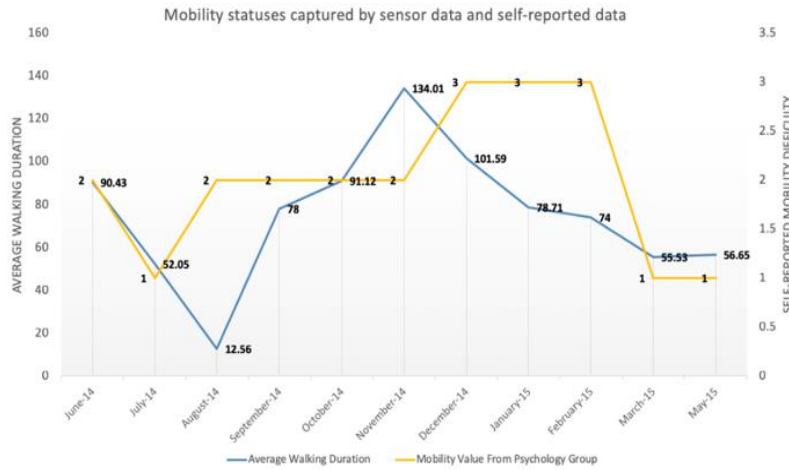


Figure 22. Compare the monthly average walking speed captured by sensor data with the self-reported mobility difficulty.

consistently drops from 3 to 1 (on a scale from 1= no difficulty to 5= tremendous difficult). The results provide evidence that the large time gaps and high frequency of Sleep and Bed-Toilet Transition activities in this particular home are related to the resident’s health status.

## 6. DISCUSSION, LIMITATIONS, AND DIRECTIONS FOR FUTURE RESEARCH

In this paper, we propose formal methods for modeling human routines in everyday environments. We found that the Pareto distribution fits many activities, thus providing unique insights into behavior norms for the entire sampled population and behavior variations between population subgroups. Further, we discover that several activities in certain groups can be described by multivariate Pareto distributions. We also explore the pattern of all activities as a routine in one home and its relationship with the resident health ailments.

When applying our analysis to smart home data, we find that activities follow a non-Poisson process and the inter-arrival times of individual activities as well as all activities within a holistic routine fit a Pareto distribution. The findings may provide useful information to further investigate potential behavior changes that might be related to health problems. Limitations of this study include sensitivity of the models to noise in the sensor data, addressed in part by the outlier filtering process. In addition, the Pareto distribution fits the data well but does not fully describe all routine details. For example, the small hump in the histogram of the data (see Fig. 11 (c)) exists with frequency in a range of 0.01 to 0.02. A mixture model may be introduced to capture the hump for greater

model detail. In Section 3, the selection of the threshold may impact the parameters of the Pareto distribution, especially when investigating the distribution’s 20% tail. However, since we look at the highest percentage of two successive activities that lie in the tail, the impact of the similar threshold/shape parameters may be small. Further, the current two subgroups only consider single residents instead of multiple residents, though the experiments that evaluate the entire 99 smart homes do include multiple residents with diverse backgrounds. The problem of tracking, recognizing, and analyzing multi-resident behavior is an ongoing challenge, although Wang et al. discuss one possible strategy for multi-resident tracking in smart homes [70].

In addition, one can observe that our initial model oversimplifies the complexity of human behavior. For the purpose of this present study, we intentionally kept the model simple and focused on automatically-detected activity timings in smart environments. However, development of more sophisticated models combining other parameters including social interactions, circadian rhythms, night time relative walking speed, and movement patterns in and out of the home can further boost our ability to understand and reproduce the structure of human activities.

Additionally, further analysis of each activity and all activities in a routine will allow us to address specific questions that have been asked in the literature. For example, we could provide evidence to support or deny the hypothesis that human behavior in certain groups is random or Markovian [71]–[74]. We could also examine whether the 80/20 rule in which the largest-distance movements (20% of movement distances) occur with 80% of total inter-arrival hours applies in home environments. Finally, future work can quantify the predictability of behavior parameters for different population groups and types of sensed data.

## 1 ACKNOWLEDGMENTS

2 This material is based upon work supported by the  
3 National Science Foundation under Grant No. 1543656.  
4 The authors would like to thank Samaneh  
5 Aminikhanghahi for her help with change point analysis.

## 7 REFERENCES

- 8 [1] G. Last and M. Penrose, *Lectures on the Poisson*  
9 *process*, vol. 7. Cambridge University Press, 2017.
- 10 [2] F. Jovan, J. Wyatt, N. Hawes, and T. Krajník, “A  
11 Poisson-spectral model for modelling temporal  
12 patterns in human data observed by a robot,” in  
13 *Intelligent Robots and Systems (IROS), 2016*  
14 *IEEE/RSJ International Conference on*, 2016, pp.  
15 4013–4018.
- 16 [3] R. G. Gallager, “Poisson processes,” *Stoch.*  
17 *Process. Theory Appl.*, pp. 74–108, 2013.
- 18 [4] A. Ihler, J. Hutchins, and P. Smyth, “Adaptive  
19 event detection with time-varying poisson  
20 processes,” in *Proceedings of the 12th ACM*  
21 *SIGKDD international conference on Knowledge*  
22 *discovery and data mining*, 2006, pp. 207–216.
- 23 [5] J. G. Oliveira and A.-L. Barabási, “Human  
24 dynamics: Darwin and Einstein correspondence  
25 patterns,” *Nature*, vol. 437, no. 7063, p. 1251,  
26 2005.
- 27 [6] A. Vázquez, J. G. Oliveira, Z. Dezsö, K. Il Goh, I.  
28 Kondor, and A. L. Barabási, “Modeling bursts and  
29 heavy tails in human dynamics,” *Phys. Rev. E -*  
30 *Stat. Nonlinear, Soft Matter Phys.*, 2006.
- 31 [7] R. F. Grais, J. H. Ellis, and G. E. Glass, “Assessing  
32 the impact of airline travel on the geographic  
33 spread of pandemic influenza,” *Eur. J. Epidemiol.*,  
34 vol. 18, no. 11, pp. 1065–1072, 2003.
- 35 [8] A. Pieropan, C. H. Ek, and H. Kjellström,  
36 “Functional object descriptors for human  
37 activity modeling,” in *Robotics and Automation*  
38 *(ICRA), 2013 IEEE International Conference on*,  
39 2013, pp. 1282–1289.
- 40 [9] O. Kwon, W.-S. Son, and W.-S. Jung, “The double  
41 power law in human collaboration behavior:  
42 The case of Wikipedia,” *Phys. A Stat. Mech. its*  
43 *Appl.*, vol. 461, pp. 85–91, 2016.
- 44 [10] L. L. Constantine, “Human activity modeling:  
45 toward a pragmatic integration of activity  
46 theory and usage-centered design,” in *Human-*  
47 *centered software engineering*, Springer, 2009,  
48 pp. 27–51.
- 49 [11] G. Gay and H. Hembrooke, *Activity-centered*  
50 *design: An ecological approach to designing*  
51 *smart tools and usable systems*. Mit Press, 2004.
- 52 [12] L. L. Constantine and L. A. D. Lockwood, *Software*  
53 *for use: a practical guide to the models and*  
54 *methods of usage-centered design*. Pearson  
55 Education, 1999.
- 56 [13] A. Bees, N. York, and A. Barabasi, “The origin of  
57 bursts and heavy tails in human dynamics,”  
58 *Nature*, vol. 435, no. 7039, pp. 207–211., 2005.
- 59 [14] J. Leskovec, M. McGlohon, C. Faloutsos, N. Glance,  
60 and M. Hurst, “Patterns of cascading behavior in  
61 large blog graphs,” in *Proceedings of the 2007*  
62 *SIAM international conference on data mining*,  
63 2007, pp. 551–556.
- 64 [15] J. Ratkiewicz, S. Fortunato, A. Flammini, F.  
65 Menczer, and A. Vespignani, “Characterizing and  
66 modeling the dynamics of online popularity,”  
67 *Phys. Rev. Lett.*, vol. 105, no. 15, p. 158701, 2010.
- 68 [16] R. Kumar, M. Mahdian, and M. McGlohon,  
69 “Dynamics of conversations,” in *Proceedings of*  
70 *the 16th ACM SIGKDD international conference*  
71 *on Knowledge discovery and data mining*, 2010,  
72 pp. 553–562.
- 73 [17] H. Li *et al.*, “Characterizing smartphone usage  
74 patterns from millions of android users,” in  
75 *Proceedings of the 2015 Internet Measurement*  
76 *Conference*, 2015, pp. 459–472.
- 77 [18] Y. Gandica, J. Carvalho, F. S. Dos Aidos, R.  
78 Lambiotte, and T. Carletti, “Stationarity of the  
79 inter-event power-law distributions,” *PLoS One*,  
80 vol. 12, no. 3, p. e0174509, 2017.
- 81 [19] I. Tsompanidis, A. H. Zahran, and C. J. Sreenan,  
82 “Mobile network traffic: A user behaviour  
83 model,” in *2014 7th IFIP Wireless and Mobile*  
84 *Networking Conference (WMNC)*, 2014, pp. 1–8.
- 85 [20] L. Yu, P. Cui, C. Song, T. Zhang, and S. Yang, “A  
86 temporally heterogeneous survival framework  
87 with application to social behavior dynamics,” in  
88 *Proceedings of the 23rd ACM SIGKDD*  
89 *International Conference on Knowledge*  
90 *Discovery and Data Mining*, 2017, pp. 1295–1304.
- 91 [21] T. M. Scholz, “The human role within  
92 organizational change: A complex system  
93 perspective,” in *Change management and the*  
94 *human factor*, Springer, 2015, pp. 19–31.
- 95 [22] P. Andriani and B. McKelvey, “Perspective—  
96 From Gaussian to Paretian thinking: Causes and  
97 implications of power laws in organizations,”  
98 *Organ. Sci.*, vol. 20, no. 6, pp. 1053–1071, 2009.
- 99 [23] Y. U. Saito, T. Watanabe, and M. Iwamura, “Do  
100 larger firms have more interfirm relationships?,”  
101 *Phys. A Stat. Mech. its Appl.*, vol. 383, no. 1, pp.  
102 158–163, 2007.
- 103 [24] M. C. Gonzalez, C. A. Hidalgo, and A.-L. Barabasi,  
104 “Understanding individual human mobility  
105 patterns,” *Nature*, vol. 453, no. 7196, pp. 779–  
106 782, 2008.
- 107 [25] I. Rhee, M. Shin, S. Hong, K. Lee, S. J. Kim, and S.  
108 Chong, “On the levy-walk nature of human  
109 mobility,” *IEEE/ACM Trans. Netw.*, vol. 19, no. 3,  
110 pp. 630–643, 2011.
- 111 [26] C. Song, Z. Qu, N. Blumm, and A.-L. Barabási,  
112 “Limits of predictability in human mobility,”  
113 *Science (80-. )*, vol. 327, no. 5968, pp. 1018–  
114 1021, 2010.
- 115 [27] W.-Y. Zhu, W.-C. Peng, L.-J. Chen, K. Zheng, and X.  
116 Zhou, “Modeling user mobility for location  
117 promotion in location-based social networks,” in  
118 *Proceedings of the 21th ACM SIGKDD*



- 1 *International Conference on Knowledge*  
2 *Discovery and Data Mining*, 2015, pp. 1573–1582.
- 3 [28] S. Hong, *Human movement patterns, mobility*  
4 *models and their impacts on wireless applications*.  
5 North Carolina State University, 2010.
- 6 [29] K. Zhao, M. Musolesi, P. Hui, W. Rao, and S.  
7 Tarkoma, “Explaining the power-law  
8 distribution of human mobility through  
9 transportation modality decomposition,” *Sci.*  
10 *Rep.*, vol. 5, p. 9136, 2015.
- 11 [30] R. Gallotti, A. Bazzani, S. Rambaldi, and M.  
12 Barthelemy, “A stochastic model of randomly  
13 accelerated walkers for human mobility,” *Nat.*  
14 *Commun.*, vol. 7, p. 12600, 2016.
- 15 [31] T. Kurashima, T. Althoff, and J. Leskovec,  
16 “Modeling interdependent and periodic real-  
17 world action sequences,” in *Proceedings of the*  
18 *2018 World Wide Web Conference on World Wide*  
19 *Web*, 2018, pp. 803–812.
- 20 [32] R. Rawassizadeh, E. Momeni, C. Dobbins, J.  
21 Gharibshah, and M. Pazzani, “Scalable daily  
22 human behavioral pattern mining from  
23 multivariate temporal data,” *IEEE Trans. Knowl.*  
24 *Data Eng.*, vol. 28, no. 11, pp. 3098–3112, 2016.
- 25 [33] N. Banovic, T. Buzali, F. Chevalier, J. Mankoff, and  
26 A. K. Dey, “Modeling and understanding human  
27 routine behavior,” in *Proceedings of the 2016 CHI*  
28 *Conference on Human Factors in Computing*  
29 *Systems*, 2016, pp. 248–260.
- 30 [34] M. Pan *et al.*, “Dissecting the Learning Curve of  
31 Taxi Drivers: A Data-Driven Approach,” in  
32 *Proceedings of the 2019 SIAM International*  
33 *Conference on Data Mining*, 2019, pp. 783–791.
- 34 [35] H. Ghayvat, J. Liu, S. C. Mukhopadhyay, and X. Gui,  
35 “Wellness sensor networks: A proposal and  
36 implementation for smart home for assisted  
37 living,” *IEEE Sens. J.*, vol. 15, no. 12, pp. 7341–  
38 7348, 2015.
- 39 [36] G. Laput, Y. Zhang, and C. Harrison, “Synthetic  
40 sensors: Towards general-purpose sensing,” in  
41 *Proceedings of the 2017 CHI Conference on*  
42 *Human Factors in Computing Systems*, 2017, pp.  
43 3986–3999.
- 44 [37] B. Lin *et al.*, “Analyzing the relationship between  
45 human behavior and indoor air quality,” *J. Sens.*  
46 *Actuator Networks*, vol. 6, no. 3, p. 13, 2017.
- 47 [38] A. P. Plageras, K. E. Psannis, C. Stergiou, H. Wang,  
48 and B. B. Gupta, “Efficient IoT-based sensor BIG  
49 Data collection–processing and analysis in  
50 smart buildings,” *Futur. Gener. Comput. Syst.*, vol.  
51 82, pp. 349–357, 2018.
- 52 [39] D. J. Cook, “Learning setting-generalized activity  
53 models for smart spaces,” *IEEE Intell. Syst.*, vol.  
54 2010, no. 99, p. 1, 2010.
- 55 [40] N. C. Krishnan and D. J. Cook, “Activity  
56 recognition on streaming sensor data,” *Pervasive*  
57 *Mob. Comput.*, vol. 10, pp. 138–154, 2014.
- 58 [41] D. Cook and N. Krishnan, “Activity Learning from  
59 Sensor Data.” Wiley, 2014.
- 60 [42] E. Kim, S. Helal, and D. Cook, “Human activity  
61 recognition and pattern discovery,” *IEEE*  
62 *pervasive Comput.*, vol. 9, no. 1, pp. 48–53, 2009.
- 63 [43] A. Benmansour, A. Bouchachia, and M. Feham,  
64 “Multioccupant activity recognition in pervasive  
65 smart home environments,” *ACM Comput. Surv.*,  
66 vol. 48, no. 3, p. 34, 2016.
- 67 [44] J. Wan, M. J. O’grady, and G. M. O’hare, “Dynamic  
68 sensor event segmentation for real-time activity  
69 recognition in a smart home context,” *Pers.*  
70 *Ubiquitous Comput.*, vol. 19, no. 2, pp. 287–301,  
71 2015.
- 72 [45] G. Fairchild, K. S. Hickmann, S. M. Mniszewski, S.  
73 Y. Del Valle, and J. M. Hyman, “Optimizing human  
74 activity patterns using global sensitivity  
75 analysis,” *Comput. Math. Organ. Theory*, vol. 20,  
76 no. 4, pp. 394–416, 2014.
- 77 [46] J. Wang, Y. Chen, S. Hao, X. Peng, and L. Hu, “Deep  
78 learning for sensor-based activity recognition: A  
79 survey,” *Pattern Recognit. Lett.*, vol. 119, pp. 3–  
80 11, 2019.
- 81 [47] A. Helal, D. J. Cook, and M. Schmalz, “Smart  
82 home-based health platform for behavioral  
83 monitoring and alteration of diabetes patients,”  
84 *J. Diabetes Sci. Technol.*, vol. 3, no. 1, pp. 141–148,  
85 2009.
- 86 [48] D. J. Cook, M. Schmitter-Edgecombe, L. Jönsson,  
87 and A. V. Morant, “Technology-enabled  
88 assessment of functional health,” *IEEE Rev.*  
89 *Biomed. Eng.*, vol. 12, pp. 319–332, 2018.
- 90 [49] C. Chen, D. J. Cook, and A. S. Crandall, “The user  
91 side of sustainability: Modeling behavior and  
92 energy usage in the home,” *Pervasive Mob.*  
93 *Comput.*, vol. 9, no. 1, pp. 161–175, 2013.
- 94 [50] S. Aminikhanghahi, T. Wang, and D. J. Cook,  
95 “Real-time change point detection with  
96 application to smart home time series data,”  
97 *IEEE Trans. Knowl. Data Eng.*, 2018.
- 98 [51] M. Yuan, “Human dynamics in space and time: A  
99 brief history and a view forward,” *Trans. GIS*, vol.  
100 22, no. 4, pp. 900–912, 2018.
- 101 [52] J. J. Davis and E. G. Conlon, “Identifying  
102 compensatory driving behavior among older  
103 adults using the situational avoidance  
104 questionnaire,” *J. Safety Res.*, vol. 63, pp. 47–55,  
105 2017.
- 106 [53] C. Li, W. K. Cheung, J. Liu, and J. K. Ng, “Automatic  
107 Extraction of Behavioral Patterns for Elderly  
108 Mobility and Daily Routine Analysis,” *ACM Trans.*  
109 *Intell. Syst. Technol.*, vol. 9, no. 5, p. 54, 2018.
- 110 [54] A. F. Costa, Y. Yamaguchi, A. J. M. Traina, and C.  
111 Faloutsos, “Modeling temporal activity to detect  
112 anomalous behavior in social media,” *ACM Trans.*  
113 *Knowl. Discov. from Data*, vol. 11, no. 4, p. 49,  
114 2017.
- 115 [55] D. J. Cook, A. S. Crandall, B. L. Thomas, and N. C.  
116 Krishnan, “CASAS: A smart home in a box,”  
117 *Computer (Long. Beach. Calif.)*, vol. 46, no. 7, pp.  
118 62–69, 2013.
- 119 [56] C. Truong, L. Oudre, and N. Vayatis, “A review of  
120 change point detection methods,” *arXiv Prepr.*

- 1 *arXiv1801.00718*, 2018.
- 2 [57] D. Picard, "Testing and estimating change-points  
3 in time series," *Adv. Appl. Probab.*, vol. 17, no. 4,  
4 pp. 841–867, 1985.
- 5 [58] S. Aminikhanghahi and D. J. Cook, "Using change  
6 point detection to automate daily activity  
7 segmentation," in *Pervasive Computing and  
8 Communications Workshops (PerCom  
9 Workshops)*, 2017 *IEEE International Conference  
10 on*, 2017, pp. 262–267.
- 11 [59] R. P. Adams and D. J. C. MacKay, "Bayesian Online  
12 Changepoint Detection," 2007.
- 13 [60] "Census Age Information." [Online]. Available:  
14 [https://www.census.gov/data/tables/2010/de  
15 mo/age-and-sex/2010-age-sex-  
16 composition.html](https://www.census.gov/data/tables/2010/demo/age-and-sex/2010-age-sex-composition.html).
- 17 [61] "Census Disability Characteristics." [Online].  
18 Available:  
19 [https://factfinder.census.gov/faces/tableservic  
20 es/jsf/pages/productview.xhtml?pid=ACS\\_16\\_1  
21 YR\\_S1810&prodType=table%0D](https://factfinder.census.gov/faces/tables/services/jsf/pages/productview.xhtml?pid=ACS_16_1_YR_S1810&prodType=table%0D).
- 22 [62] "Census Educational Information." [Online].  
23 Available:  
24 [https://www.census.gov/data/tables/2010/de  
25 mo/educational-attainment/cps-detailed-  
26 tables.html%0D](https://www.census.gov/data/tables/2010/demo/educational-attainment/cps-detailed-tables.html%0D).
- 27 [63] "Census Households Information." [Online].  
28 Available:  
29 [https://www.census.gov/data/tables/time-  
30 series/demo/families/households.html%0D](https://www.census.gov/data/tables/time-series/demo/families/households.html%0D).
- 31 [64] S. Coles, J. Bawa, L. Trenner, and P. Dorazio, *An  
32 introduction to statistical modeling of extreme  
33 values*, vol. 208. Springer, 2001.
- 34 [65] V. Hodge and J. Austin, "A survey of outlier  
35 detection methodologies," *Artif. Intell. Rev.*, vol.  
36 22, no. 2, pp. 85–126, 2004.
- 37 [66] R. J. Hyndman, "The problem with Sturges' rule  
38 for constructing histograms," *Monash Univ.*, no.  
39 July, pp. 1–2, 1995.
- 40 [67] Ž. Ivezić, A. J. Connolly, J. T. VanderPlas, and A.  
41 Gray, *Statistics, Data Mining, and Machine  
42 Learning in Astronomy: A Practical Python Guide  
43 for the Analysis of Survey Data*. Princeton  
44 University Press, 2014.
- 45 [68] I. Salgado-Ugarte, M. Shimizu, and T. Taniuchi,  
46 "Practical rules for bandwidth selection in  
47 univariate density estimation," *Stata Tech. Bull.*,  
48 vol. 5, no. 27, pp. 5–19, 1995.
- 49 [69] D. Freedman and P. Diaconis, "On the histogram  
50 as a density estimator:L2 theory," *Zeitschrift für  
51 Wahrscheinlichkeitstheorie und Verwandte  
52 Gebiete*, vol. 57, no. 4, pp. 453–476, 1981.
- 53 [70] D. J. C. Tinghui Wang, "Towards Unsupervised  
54 Multi-Resident Tracking in Ambient Assisted  
55 Living: Methods and Performance Metrics," in  
56 *Assistive Technology for the Elderly, 1st Edition*, N.  
57 S. Subhas Mukhopadhyay, Ed. Academic Press.
- 58 [71] M. Rosenblatt, *Markov Processes, Structure and  
59 Asymptotic Behavior: Structure and Asymptotic  
60 Behavior*, vol. 184. Springer Science & Business  
61 Media, 2012.
- 62 [72] K. Doty, S. Roy, and T. R. Fischer, "Filtering and  
63 smoothing state estimation for flag Hidden  
64 Markov Models," in *American Control Conference  
65 (ACC), 2016*, 2016, pp. 7042–7047.
- 66 [73] M. Xue and S. Roy, "Spectral and graph-theoretic  
67 bounds on steady-state-probability estimation  
68 performance for an ergodic Markov chain," *J.  
69 Franklin Inst.*, vol. 348, no. 9, pp. 2448–2467,  
70 2011.
- 71 [74] S. Roy, "Scaled consensus," *Automatica*, vol. 51,  
72 pp. 259–262, 2015.
- 73